OPEN ACCESS Freely available online

PLOS ONE

Hysteresis Responses of Evapotranspiration to Meteorological Factors at a Diel Timescale: Patterns and Causes

Han Zheng[1,3], Qiufeng Wang[1]*, Xianjin Zhu[1,3], Yingnian Li[2], Guirui Yu[1]*

1 Synthesis Research Center of Chinese Ecosystem Research Network, Key Laboratory of Ecosystem Network Observation and Modeling, Institute of Geographic Sciences and Natural Resources Research, Chinese Academy of Sciences, Beijing, China, **2** Northwest Institute of Plateau Biology, Chinese Academy of Sciences, Xining, China, **3** University of Chinese Academy of Sciences, Beijing, China

Abstract

Evapotranspiration (ET) is an important component of the water cycle in terrestrial ecosystems. Understanding the ways in which ET changes with meteorological factors is central to a better understanding of ecological and hydrological processes. In this study, we used eddy covariance measurements of ET from a typical alpine shrubland meadow ecosystem in China to investigate the hysteresis response of ET to environmental variables including air temperature (T_a), vapor pressure deficit (VPD) and net radiation (R_n) at a diel timescale. Meanwhile, the simulated ET by Priestly-Taylor equation was used to interpret the measured ET under well-watered conditions. Pronounced hysteresis was observed in both T_a and VPD response curves of ET. At a similar T_a and VPD, ET was always significantly depressed in the afternoon compared with the morning. But the hysteresis response of ET to R_n was not evident. Similar hysteresis patterns were also observed in the T_a/VPD response curves of simulated ET. The magnitudes of the measured and simulated hysteresis loops showed similar seasonal variation, with relatively smaller values occurring from May to September, which agreed well with the lifetime of plants and the period of rainy season at this site. About 62% and 23% of changes in the strength of measured ET-T_a and ET-VPD loops could be explained by the changes in the strength of simulated loops, respectively. Thus, the time lag between R_n and T_a/VPD is the most important factor generating and modulating the ET-T_a/VPD hysteresis, but plants and water status also contribute to the hysteresis response of ET. Our research confirmed the different hysteresis in the responses of ET to meteorological factors and proved the vital role of R_n in driving the diel course of ET.

Citation: Zheng H, Wang Q, Zhu X, Li Y, Yu G (2014) Hysteresis Responses of Evapotranspiration to Meteorological Factors at a Diel Timescale: Patterns and Causes. PLoS ONE 9(6): e98857. doi:10.1371/journal.pone.0098857

Editor: Gil Bohrer, The Ohio State University, United States of America

Received January 9, 2014; **Accepted** May 8, 2014; **Published** June 4, 2014

Funding: This research was jointly supported by Key program of National Natural Science Foundation of China (Grant NO. 31290221), National Basic Research Program (Grant NO. 2010CB833504), and Remote Sensing Investigation and Assessment on National Ecological Environment Decade Changes (2000–2010) program (STSN-02-02). The funders had no role in study design, data collection and analysis, decision to publish, or preparation of the manuscript.

Competing Interests: The authors have declared that no competing interests exist.

* E-mail: qfwang@igsnrr.ac.cn (QW); yugr@igsnrr.ac.cn (GY)

Introduction

Evapotranspiration (ET), an important component of the water cycle and the principal route of water loss in terrestrial ecosystems, strongly affects biogeochemical cycles and the surface energy balance and further influences the local weather and climate [1,2]. A number of environmental variables (e.g., net radiation, vapor pressure deficit, air temperature, wind speed and soil water content) have significant impacts on the variability of ET, whereas the dominant factor varies at different spatiotemporal scales [2–7]. Therefore, analyzing the responses of ET to environmental variables is of great significance to achieve a better understanding of the water cycle.

Hysteresis between transpiration (or sap flow) and microclimate variables (mainly VPD) has been widely reported on the basis of individual plants or even more small units (e.g., tree branches) [8–15]. As we know, ET is generally parameterized as the sum of vegetation transpiration and soil evaporation [2,16]. Accordingly, the response patterns of ET to environmental factors are the integrated consequences of all processes and parameters influencing transpiration and evaporation. The dominance of transpiration in terrestrial ET [17] suggests that hysteresis might occur in responses of ET to environmental factors. To our knowledge, however, only a few studies [18–20] reported the hysteresis phenomenon in the response of ET to photosynthetically active radiation (PAR) or VPD. As these results were based on quite short-term data and only one environmental factor was considered, the consistency of hysteresis at a long-term scale remains to be questioned and more environmental factors should be taken into account if a more complete understanding of the ecosystem water cycle and its response mechanisms to environmental variables is desired.

Alpine meadows are characterized by relatively high precipitation, strong solar radiation and low temperature [21] and are very sensitive and vulnerable to global climate change [22], providing a special opportunity to examine ecosystem ET in response to changes in environmental conditions. The eddy covariance (EC) method continuously monitors water flux between the ecosystem and atmosphere and associated environmental factors, facilitating the analysis of the response patterns of ET to environmental factors [23]. In the present study, we used the EC flux measurements from a typical alpine shrubland meadow ecosystem,

a component of the Chinese Terrestrial Ecosystem Flux Research Network (ChinaFLUX), during 2003–2011 to investigate the diel course of ET and its response patterns to key environmental factors including air temperature (T_a), vapor pressure deficit (VPD) and net radiation (R_n) at a diel timescale. This research seeks to answer the following scientific questions: (1) Is hysteresis observed in the response of ET to environmental factors at a diel timescale (24 h)? (2) To which environmental factor(s) does ET respond with strong hysteresis? (3) What are the seasonal patterns of hysteresis? and (4) What are the potential causes of hysteresis and of its seasonal variation?

Materials and Methods

Site Description

The study site is a component of the ChinaFLUX network and is classified as an alpine shrubland meadow. It is located at the Haibei Research Station, Chinese Academy of Sciences, in Qinghai Province, China (latitude 37°39′55″N, longitude 101°19′52″E, altitude 3293 m). The site is located on the northeastern Qinghai-Tibetan Plateau and experiences a typical plateau continental climate with long, cold winters and short, cool summers. Climate data show that the annual average air temperature and amount of annual precipitation are −1.6°C and 560 mm, respectively (data from 1980 to 2001 from the Haibei climate station). Approximately 80% of the annual rainfall falls within the rainy season, which is also the growing season, extending from May to September [24]. The soil type is Mollic-Cryic Cambisols [25], with rich organic content and a thin soil layer. The vegetation is dominated by *Dasiphora fruticosa* and reaches a height of 30–40 cm. Many herbaceous plants with mean heights of 8–20 cm grow in the meadow; the dominant species are *Helictotrichon tibeticum* and *Elymus nutans*. The vegetation at the study site starts to green at the end of April or early May and begins to senesce in late September or early October depending on the

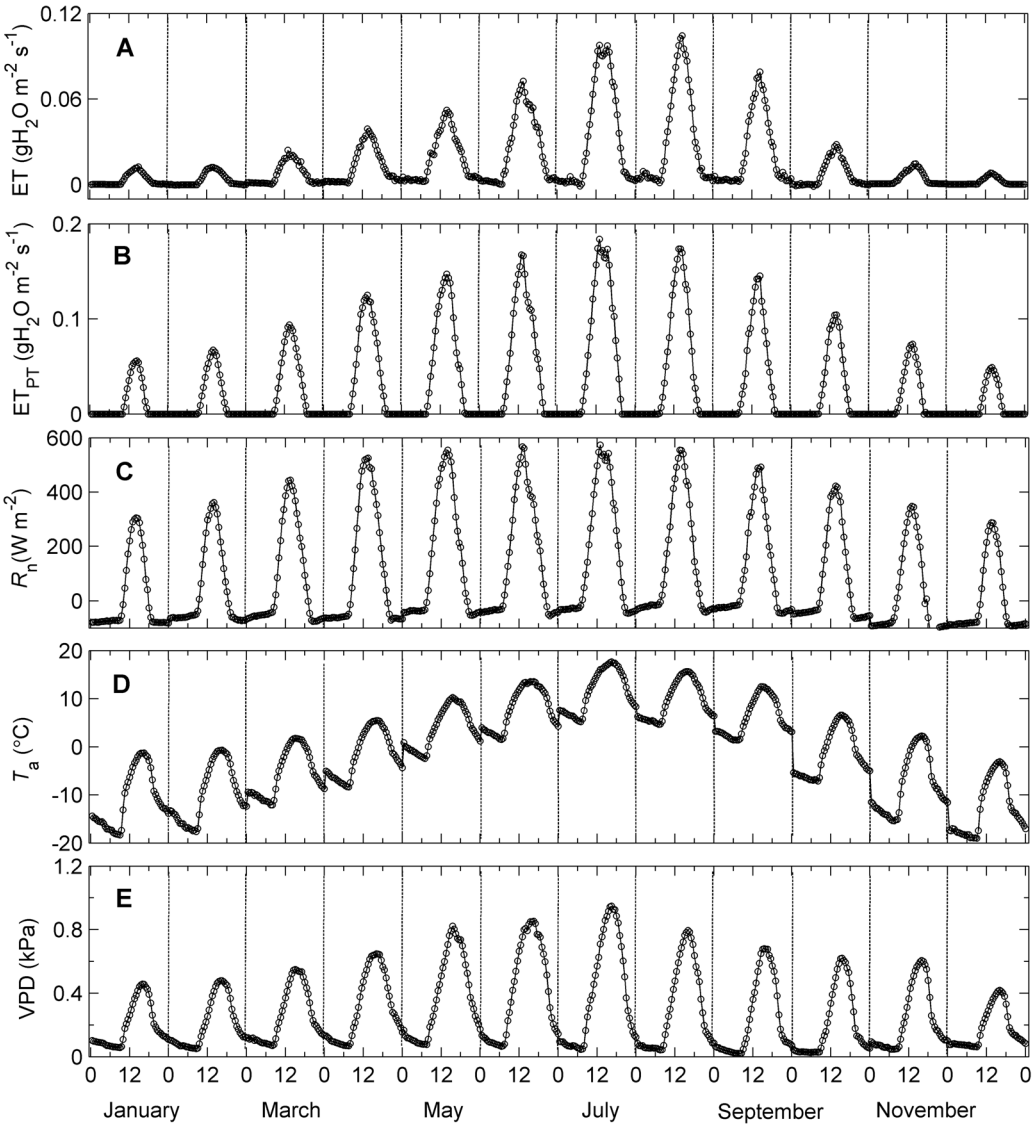

Figure 1. Diel patterns of evapotranspiration (ET) measured by eddy covariance method (A), calculated ET using Priestly-Taylor equation (ET_{PT}, B), net radiation (R_n, C), air temperature (T_a, D), and vapor pressure deficit (VPD, E). Data points are half-hourly values averaged monthly during 2010. BST is depicted in the upper *x axis* (0 = midnight, 12 = noon), and month is depicted in the lower *x axis*.
doi:10.1371/journal.pone.0098857.g001

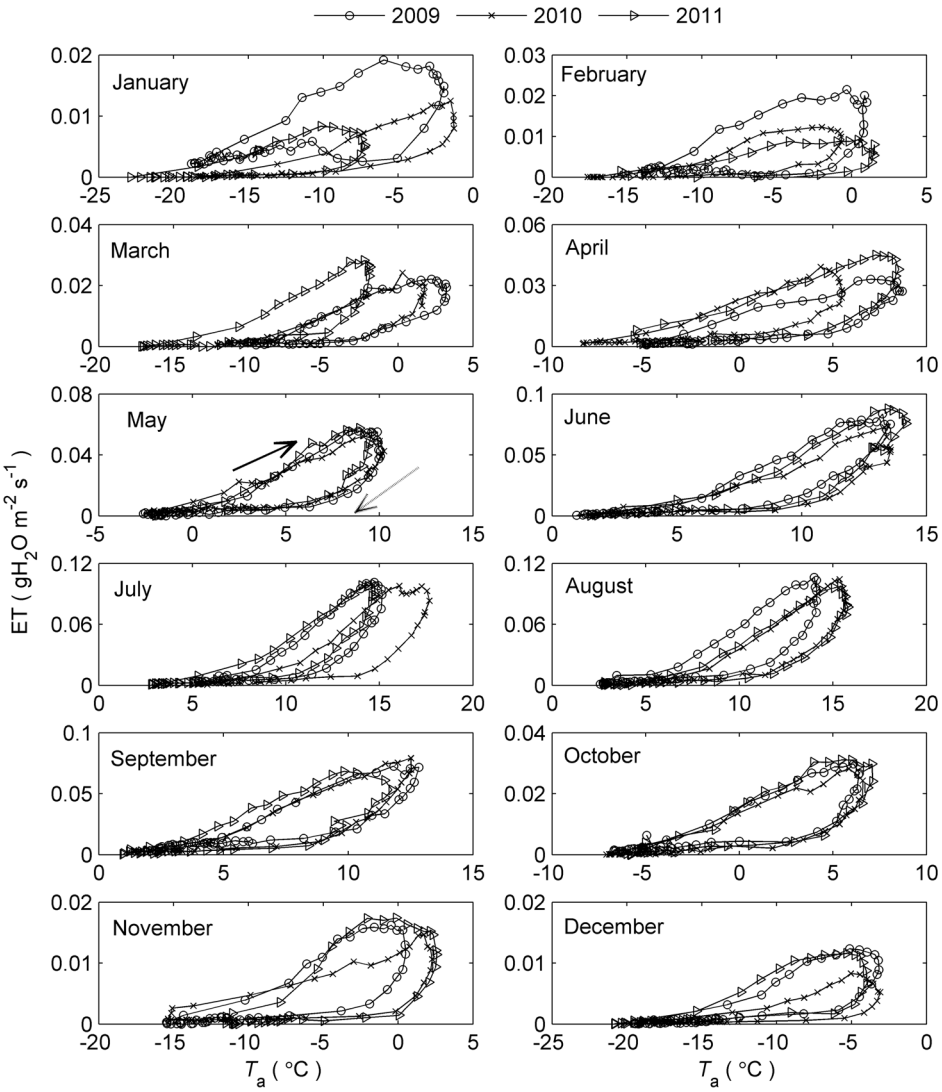

Figure 2. Temperature response curves of ET at diel timescale. Data points are half-hourly values averaged monthly. The solid arrows indicate the direction of response in the morning and the dashed ones indicate the direction of response in the afternoon. The area enclosed by the ET trajectories measures the strength of the hysteresis loop.
doi:10.1371/journal.pone.0098857.g002

meteorological conditions of the given year. More detailed site information is available in previous studies [25].

Measurements

Water vapor flux and micrometeorological conditions were measured since September 2002. The EC system was composed of a three-dimensional sonic anemometer (CSAT3, Campbell, USA) and an open-path fast response infrared CO_2/H_2O analyzer (Li-7500, Li-Cor Inc, USA). The sensors were mounted at a height of 2.2 m above the ground with a fetch of more than 250 m in all directions [26]. The EC measurements were sampled with a frequency of 10 Hz and then recorded with a data logger at 30-min intervals. Meteorological variables, including R_n, T_a, incident solar radiation (R_s) and relative humidity (RH), were measured and calculated simultaneously at 30-min intervals. VPD was calculated from the observations of T_a and RH. Further details of the monitoring system were presented by Zhao *et al.* (2005) [26]. The energy closure ratio of this site exceeded 0.7 [27], indicating reasonable data quality.

Data Processing

To process the raw 30-min flux data, we applied the routine processing procedures recommended by ChinaFLUX, including three-dimensional coordinate rotation, WPL (Webb-Pearman-Leuning) correction, removal of anomalous values and gap filling [28]. The three-dimensional rotation was applied to make the average vertical wind speed to zero and to force the horizontal wind to the mean wind direction. WPL correction was used to adjust the effect of density change on CO_2 and H_2O fluxes (Webb *et al.*, 1980) [29].

Spurious data caused by rainfall, water condensation or system failure were removed from the dataset. To exclude the low turbulence fluxes at night, the friction velocity (u*) threshold was calculated according to Reichstein et al (2005) [30] as follows: Firstly, every three months data were grouped into one set and each year data were divided into four sets. Secondly, in each set, all available data were split into six subsets having the same sample size and the similar temperature. In each subset, data were divided into 20 classes by u*. The threshold of u* in this subset was defined

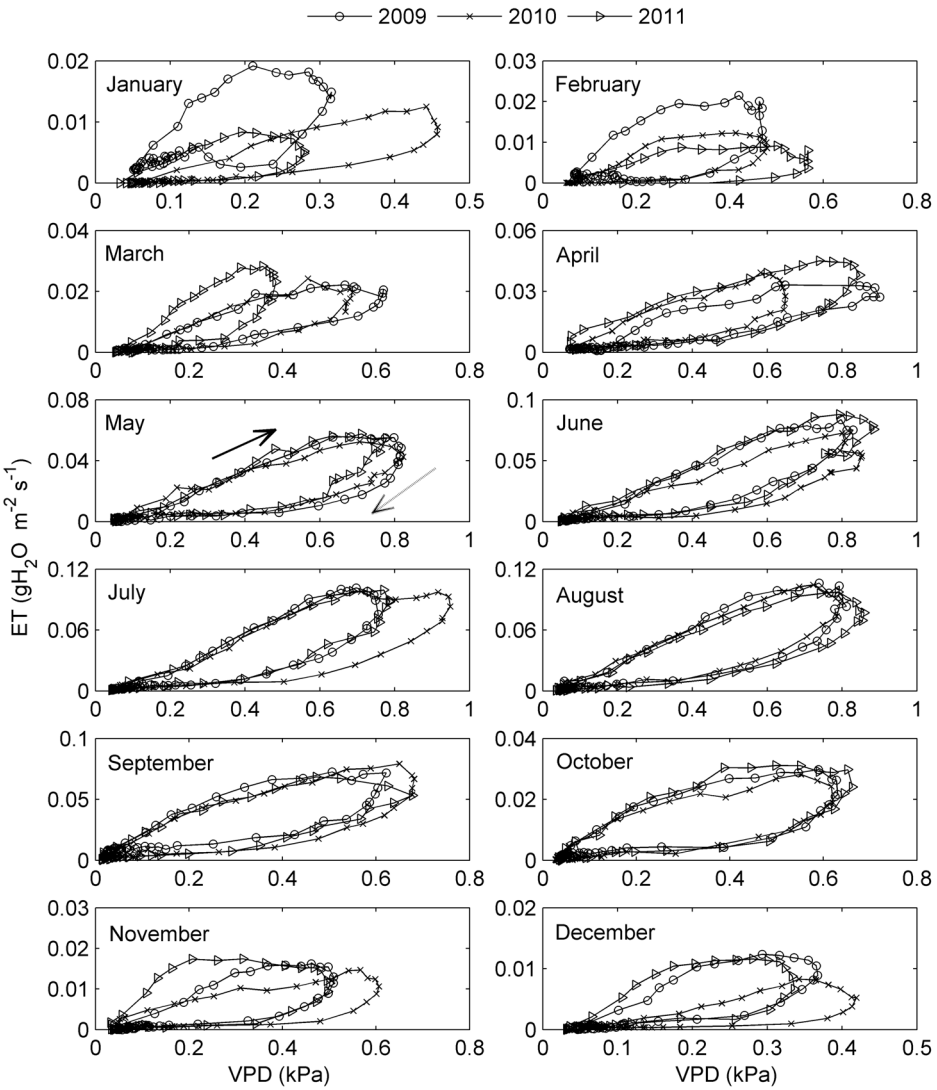

Figure 3. Vapor pressure deficit response curves of ET at diel timescale. Data points are half-hourly values averaged monthly. The solid arrows indicate the direction of response in the morning and the dashed ones indicate the direction of response in the afternoon. The area enclosed by the ET trajectories measures the strength of the hysteresis loop.
doi:10.1371/journal.pone.0098857.g003

as the u* value where the carbon flux was higher than the 95% of the average flux at the higher u* class. The threshold of u* for each set was calculated as the median of the u* threshold from six subsets. Then the u* threshold for the whole dataset was set as the highest threshold found.

Data gaps due to missing or rejected data are unavoidable in long-term and continuous measurements. We filled short gaps (< 2 h) in the water flux data with linear interpolation, and we applied a look-up table method for the longer gaps [30,31] using T_a, VPD and R_s. For the meteorological data, we used linear interpolation for gaps of less than 2 h and the mean diurnal variation method for the longer gaps [31]. All the data processing procedures specified above were performed with a Matlab program written in-house.

ET Calculated by Priestly-Taylor Equation

To assess the effects of time lag between R_n and T_a/VPD on the ET-T_a/VPD hysteresis, Priestly-Taylor (P-T) equation, which is a simple ET model driven by only R_n and T_a, was used in this study. Under well-watered conditions, P-T equation can be written as [2,32]:

$$\mathrm{ET_{PT}} = \alpha \frac{\Delta(R_n - G)}{(\Delta + \gamma)\lambda}$$

where $\mathrm{ET_{PT}}$, the ET calculated by P-T equation ($gH_2O\ m^{-2}\ s^{-1}$), could be used to interpret eddy covariance measurements in well watered conditions; α, the Priestly-Taylor coefficient, is given as 1.26 for wet or humid conditions in this study; Δ is the slope of relation between saturation vapor pressure and temperature (kPa $^{\circ}C^{-1}$); γ is the psychrometric constant (kPa $^{\circ}C^{-1}$); R_n and G are net radiation and soil heat flux (W m^{-2}), respectively; and λ is the latent heat of vaporization (2.45 MJ kg^{-1}). When nighttime PAR was smaller than 10 μmol photon $m^{-2}s^{-1}$ or the P-T model prediction was negative, the P-T simulations for ET were set to zero in this study.

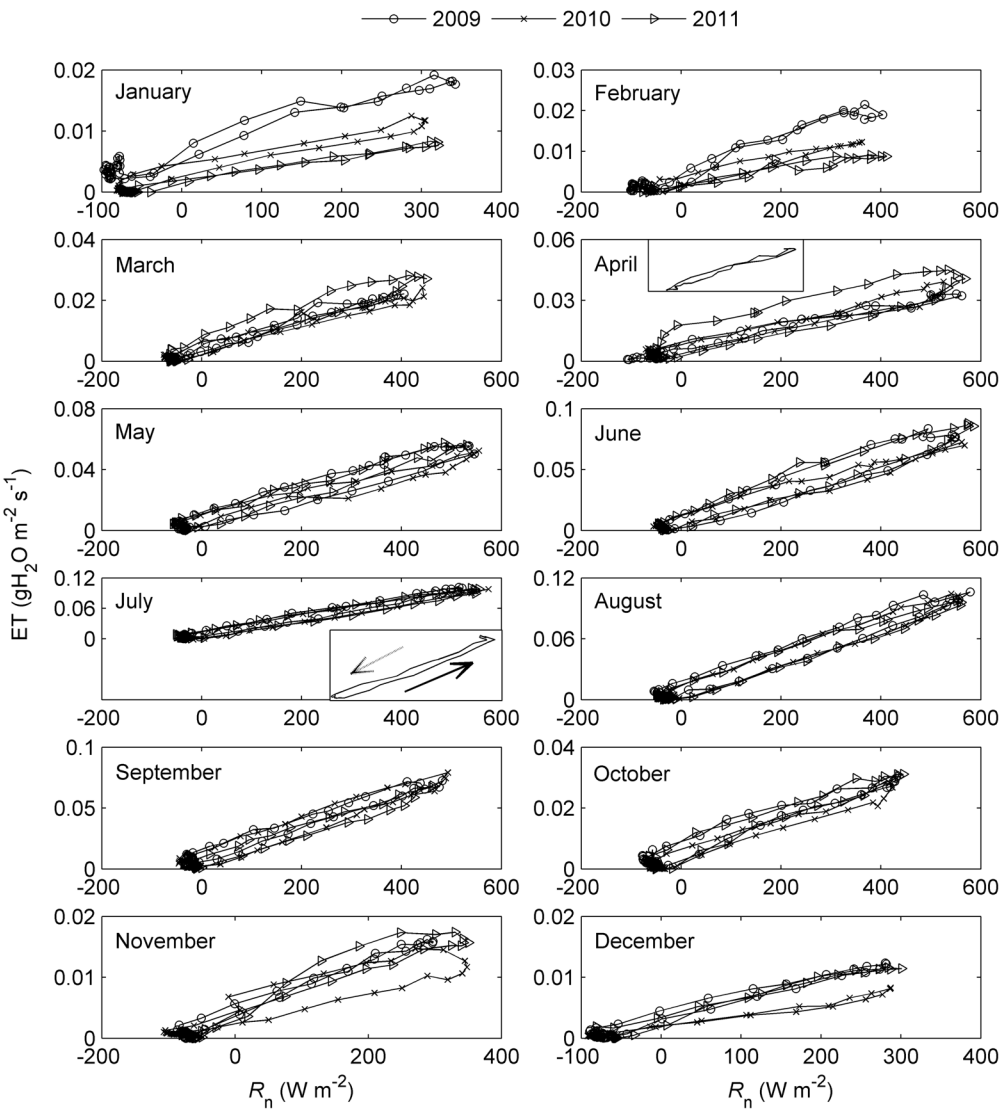

Figure 4. Net radiation response curves of ET at diel timescale. Data points are half-hourly values averaged monthly. The thumbnails in subplots 'April' and 'July' are R_n response curves in April of 2009 and July of 2010, respectively. The solid arrow indicates the direction of response in the morning and the dashed one indicates the direction of response in the afternoon.
doi:10.1371/journal.pone.0098857.g004

Data Analyses

Monthly averaged 30-min values of ET and relevant meteorological variables (including T_a, VPD and R_n) collected from 2003 to 2011 were analyzed. The monthly averaged values were calculated by averaging each 30-min datum for a particular time over 1 month. ET was then plotted against each of the corresponding T_a, VPD and R_n datasets. Monthly averaged 30-min data for ET, T_a, VPD and R_n from 2009 to 2011 are available in Table S1.

All the response curves plots specified above consisted of two parts: an increasing part, in which ET increased with changes in T_a/VPD/R_n, and a decreasing part, in which ET decreased with changes in T_a/VPD/R_n. In this study, we defined the increasing part as 'morning' and the decreasing part as 'afternoon'. We used a t-test to analyze the significance of the hysteretic relationship between the morning and afternoon during one day. The difference was considered significant if $P<0.05$.

To illustrate the month-to-month variation in hysteresis, normalized plots were used to remove the influence of the magnitudes of ET and T_a/VPD from the data. In a normalized plot, the proportion of maximum ET of the specific month was plotted against the proportion of maximum T_a or the proportion of maximum VPD. Here, T_a is absolute temperature converted by the measured centigrade temperature by adding 273.15. Then the area within the normalized hysteresis loop (H_{area}) was computed with a built-in function named *Polyarea* in Matlab R2009a to quantify the strength of hysteresis. The normalized plots were also used to compare the differences of ET-VPD (and ET-T_a) hysteresis between the EC measurements and P-T calculations. A simple regression was used to analyze the relationship between the EC H_{area} and P-T H_{area}, which was considered significant if $P<0.05$. All the statistical analyses were performed with SPSS 16.0 for Windows, and all figures were plotted using Matlab R2009a.

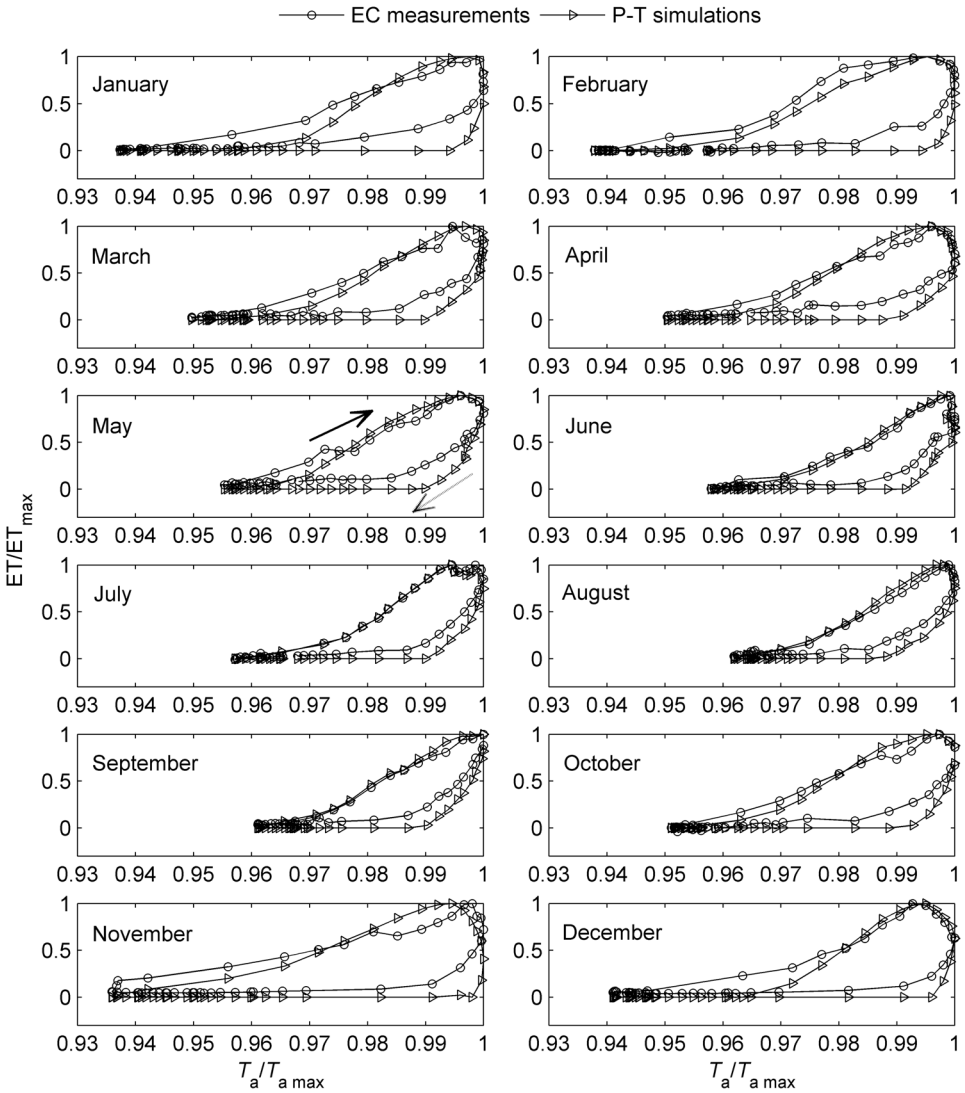

Figure 5. An example of seasonal variation in ET-T_a hysteresis using normalized plots in 2010. The *y axis* represents the proportion of maximum ET (dimensionless) and the *x axis* represents the proportion of maximum T_a (dimensionless). Here, T_a is absolute temperature (K) converted by the measured centigrade temperature (°C) by adding 273.15. The solid arrow indicates the direction of response in the morning and the dashed one indicates the direction of response in the afternoon. The area enclosed by the ET trajectories measures the strength of the hysteresis loop.
doi:10.1371/journal.pone.0098857.g005

Results

Diel Patterns of ET and Meteorological Factors

The monthly averaged diel patterns of measured ET by eddy covariance method and model-calculated ET using Priestly-Taylor equation (ET_{PT}) were markedly unimodal during almost every month (Figure 1A and 1B). The ET values during the night were low and showed small changes, then rapidly increased and peaked at approximately 13:00–14:00 Beijing Standard Time (BST, approximately 1 h earlier than the solar time at the study site). ET then began to decline and approached zero at approximately 18:00–20:00 BST (depending on the season). R_n, VPD and T_a also presented similar diel trends (Figure 1C, 1D and 1E) and R_n was almost in phase with both measured and simulated ET. R_n attained its peak values at approximately the same time as ET, whereas the peak values of T_a and VPD lagged well behind ET for almost 2 h.

The Relationship between ET and Meteorological Factors

Distinct clockwise hysteresis loops were observed in the relationship between ET and T_a for all diel cycles averaged monthly from 2003 to 2011 (Figure 2, Figure S1 and Figure S2). As T_a increased in the morning, ET increased and peaked at an optimum temperature. ET then declined with decreasing T_a in the afternoon. However, at the same temperature, ET was always higher in the morning than in the afternoon, forming a significant clockwise hysteresis loop ($P<0.05$ for all months except October 2007). Obvious clockwise hysteresis loops were also observed in the VPD response curves of ET (Figure 3, Figure S3 and Figure S4). Specifically, the morning values of ET were greater than the afternoon values of ET at any given value of VPD ($P<0.05$ for all months except October 2007). The trend in the variation of the R_n response curves of ET was similar to that of the T_a and VPD response curves (Figure 4, Figure S5 and Figure S6), with anti-clockwise loops observed for many months (e.g., Figure 4-July). However, the hysteresis was much weaker than that of the ET-T_a

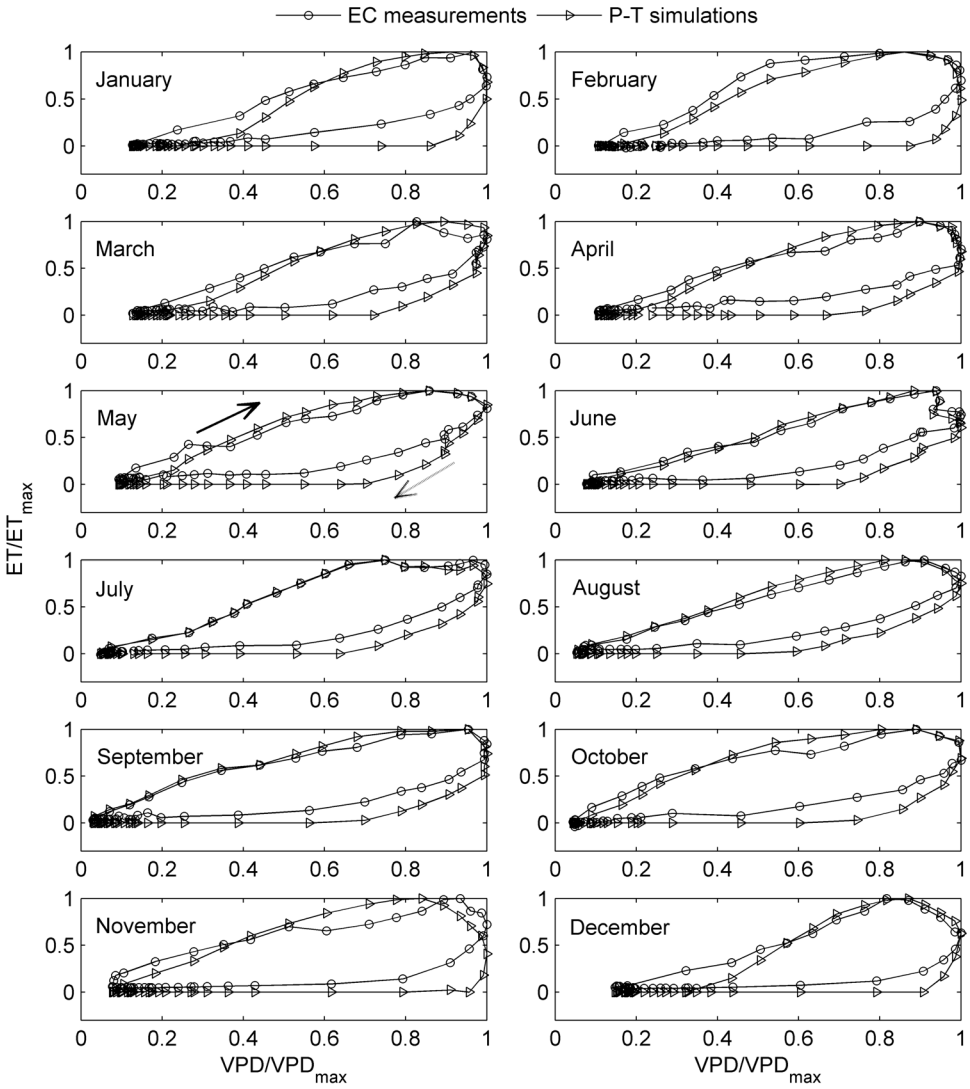

Figure 6. An example of seasonal variation in ET-T_a hysteresis using normalized plots in 2010. The *y axis* represents the proportion of maximum ET (dimensionless) and the *x axis* represents the proportion of maximum VPD (dimensionless).The solid arrow indicates the direction of response in the morning and the dashed one indicates the direction of response in the afternoon. The area enclosed by the ET trajectories measures the strength of the hysteresis loop.
doi:10.1371/journal.pone.0098857.g006

and ET-VPD relationships ($P>0.05$ for all months except April 2009 and July 2010). The patterns of the incident solar radiation (R_s) response curves were similar to those of the R_n response curves, with no significant hysteresis detected (figure not shown).

All the T_a/VPD/R_n response curves of simulated ET using P-T equation also exhibited similar trend with the corresponding curves of the measured ET, i.e., pronounced ET-T_a and ET-VPD hysteresis (Figure 5 and Figure 6) while no distinct hysteresis in ET-R_n relationship (Figure not shown). Moreover, most of the time, the simulated loops were larger than the measured ones, however, their upper parts (i.e., in the morning) nearly overlapped during many months (Figure 5 and Figure 6).

Seasonal Patterns of ET-T_a and ET-VPD Hysteresis

Although the clockwise hysteresis pattern was highly consistent in both the T_a and VPD response curves of ET, the degree of the hysteresis loops differed substantially among the months during the year. An example of the seasonal variation in ET-T_a and ET-VPD hysteresis is presented in Figure 5 and Figure 6, respectively, using normalized plots to remove the influence of the magnitudes of ET and T_a/VPD from the data. There was pronounced month-to-month variation in hysteresis, especially in ET-T_a hysteresis (Figure 5). The seasonal patterns of ET hysteresis were quite similar during the nine years, though subtle differences existed (Figure 7). In general, both the magnitudes of the ET-T_a and ET-VPD hysteresis (manifested by the area within the hysteresis loop, H_{area}) were relatively small from May to September (Figure 7).

At the meantime, the patterns of variation in the simulated ET hysteresis by P-T equation agreed very well with that of the measured hysteresis in both VPD and T_a situations among the observation period (Figure 7). Simple regression analyses demonstrated that H_{area} of simulated ET-T_a and ET-VPD loops could explain about 62% and 23% of changes in that of measured loops, respectively (Figure 8). Meanwhile, the simulated H_{area} was virtually always bigger than the measured H_{area}, but the gaps between simulated H_{area} and measured H_{area} were not nearly

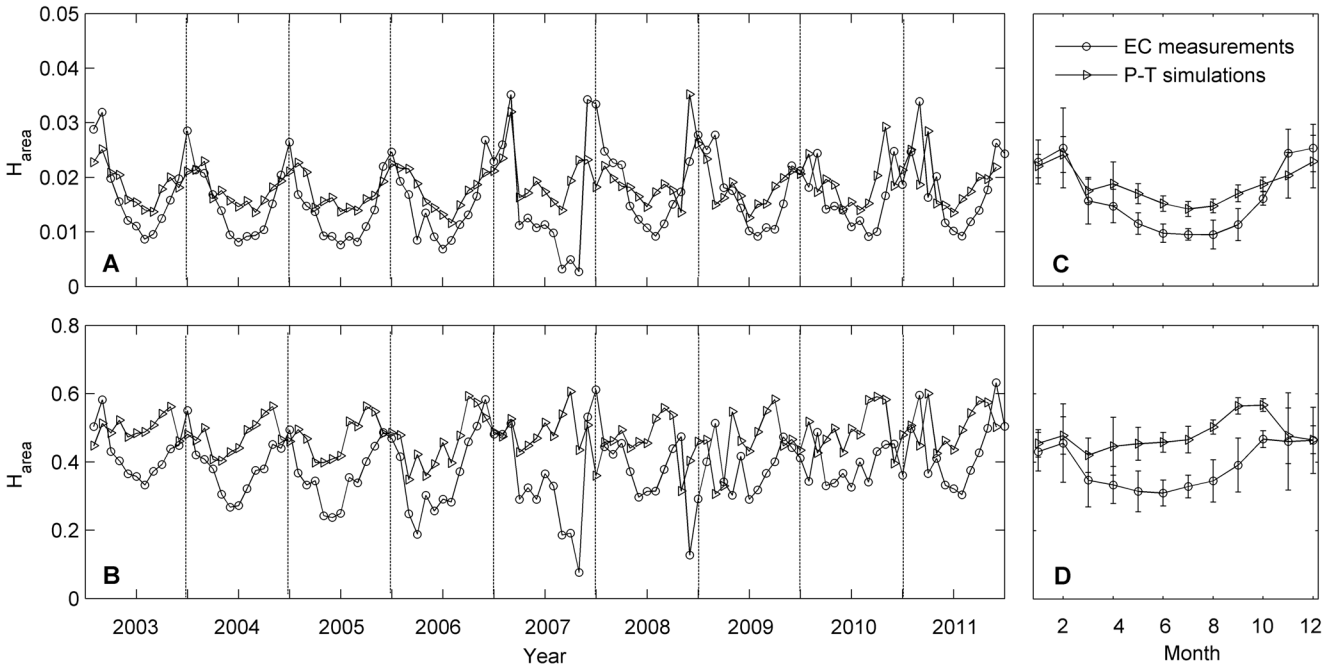

Figure 7. Seasonal variation in ET-T_a (A and C) and ET-VPD (B and D) hysteresis area from 2003 to 2011. Each data point in the left panels represents the hysteresis area (H_{area}) for a month, while each data point in the right panels represents a multi-year average of H_{area} (mean ± 1SE) for a particular month from 2003 to 2011 (datum in October 2007 was eliminated). H_{area} is calculated from normalized plot (e.g., Figure 5 and Figure 6).
doi:10.1371/journal.pone.0098857.g007

equal through the year, but with relatively larger gaps from May to September (Figure 7).

Discussion

Hysteresis in ET-T_a and ET-VPD Relationships

In this study, diel patterns of ET were almost in phase with that of R_n, while phase differences existed between T_a/VPD and R_n (Figure 1). Thus, the time lag between R_n and T_a/VPD might be an important factor generating the ET-VPD hysteresis, because R_n is the primary driver for evaporation. To assess this, simulated ET by Priestly-Taylor equation for a well-watered surface was used to remove the influence of real water status of plants. It turned out that the looping patterns showed up in both the measured and calculated ET-T_a/VPD relationships (Figure 5 and Figure 6), which demonstrated the vital role of the time lag between R_n and T_a/VPD in forming the ET-T_a/VPD hysteresis loops.

Since the role of plant water status of the study site has not been considered in the P-T equation, the measured and calculated ET-T_a/VPD hysteresis loops were not exactly the same in our research. For example, overlaps were observed between the measured and simulated hysteresis loops in the morning (Figure 5

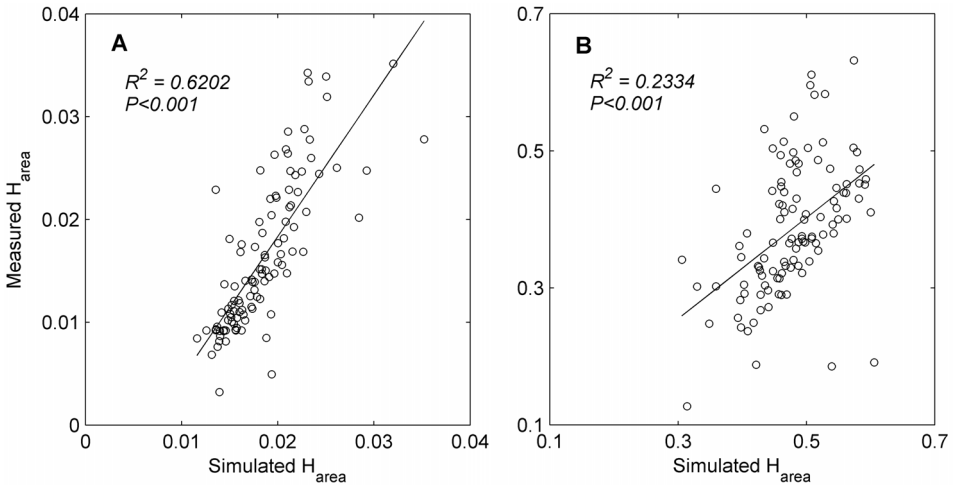

Figure 8. Relationship between the area within the measured and simulated hysteresis loops. Panel A and B are with respect to ET-T_a and ET-VPD relation, respectively. H_{area} is calculated from normalized plot (e.g., Figure 5 and Figure 6).
doi:10.1371/journal.pone.0098857.g008

and Figure 6). This is because the water supply capacity of the plants and even the soil in the morning is larger than that in the afternoon. In the morning, water may even be secreted from the hydathodes at the top or margin of the leaves [33] following rehydration at night. In contrast, plants may be partially dehydrated in the afternoon [9,12,14]. Dew appearing on exposed surfaces of the plants and the soil in the morning or evening due to condensation will also most likely contribute to increase the water supply capacity and hence produce a higher ET in the morning than in the afternoon.

Besides, the opening/closing behavior of stomata might also contribute to the emergence of hysteresis. Previous studies found that stomata responded differently to changes in environmental factors (e. g., VPD) during the processes of stomatal opening and closing, with larger stomatal conductance in the morning [34,35], indicating higher canopy conductance [36] and hence higher ET in the morning compared with the afternoon.

Seasonal Variation in ET-T_a and ET-VPD Hysteresis

Pronounced seasonal variation has been observed in both the measured and simulated ET hysteresis in our study, with relatively small magnitudes (manifested by the area within the hysteresis loop, H_{area}) from May to September (Figure 7). As indicated by our simple regression analyses, changes in the simulated H_{area} of simulated ET-T_a and ET-VPD loops could explain approximately 62% and 23% of changes in that of measured loops, respectively (Figure 8). That's to say, the variation in the phase difference (or time lag) between R_n and T_a/VPD is an important factor modulating the strength of ET-T_a/VPD hysteresis, though it is not clear yet why the relation between the magnitudes of simulated and measured loops is stronger in the ET-T_a relationship.

Gaps existed between the simulated and measured curves of H_{area}, which is easy to understand. However, the gaps were not nearly equal through the year, but with relatively larger gaps from May to September, which agrees well with the lifetime of plants and also the period of rainy season at this study site. Hence, we speculate that the development of canopy and the water status of this ecosystem might have weakened the degree of ET hysteresis during the large-gap period, i.e., from May to September. But it is still unclear how plants and water status regulate the strength of hysteresis, which may be deeply investigated in future.

Hysteresis Responses of ET to Meteorological Factors

Pronounced clockwise hysteresis loops were consistently rather than accidentally observed in the ET-T_a and ET-VPD relationships at a diel timescale based on the nine-year observations of the alpine shrubland meadow ecosystem (Figure 2 and Figure 3). This hysteresis phenomenon of ET was similar to that of transpiration in response to VPD, as documented in several previous studies (e.g., [10,12,13,15]). These results indicate that the diel patterns of ET in response to VPD and T_a agree well with the diel response patterns of vegetation transpiration. Similarly, several researchers have also observed diel hysteresis patterns between transpiration and R_s (or PAR) [8,10,11,15], with loops that were anti-clockwise [10] or in totally opposite directions before and after rainfall [15]. However, the diel hysteresis response between ET and R_n found in this study was not significant, although small anti-clockwise loops occurred frequently (Figure 4). This result might illustrate the differences between the characteristics of the responses of ET and transpiration to solar radiation.

The hysteresis responses of ET to T_a/VPD indicate that using T_a or VPD to simply simulate ET may induce certain uncertainties, while we can conservatively believe that based on the R_n data, a simple model can be obtained to simulate the diel variation of ET.

Supporting Information

Figure S1 Temperature response curves of ET at diel timescale from 2003 to 2005.
(TIF)

Figure S2 Temperature response curves of ET at diel timescale from 2006 to 2008.
(TIF)

Figure S3 Vapor pressure deficit response curves of ET at diel timescale from 2003 to 2005.
(TIF)

Figure S4 Vapor pressure deficit response curves of ET at diel timescale from 2006 to 2008.
(TIF)

Figure S5 Net radiation response curves of ET at diel timescale from 2003 to 2005.
(TIF)

Figure S6 Net radiation response curves of ET at diel timescale from 2006 to 2008.
(TIF)

Table S1 Monthly averaged half-hourly data for evapotranspiration, air temperature, vapor pressure deficit and net radiation from 2009 to 2011.
(XLS)

Acknowledgments

We gratefully thank the editor and two anonymous reviewers' valuable comments and constructive suggestions on the previous version of the manuscript.

Author Contributions

Conceived and designed the experiments: HZ QW GY. Performed the experiments: HZ QW GY. Analyzed the data: HZ QW XZ GY. Contributed reagents/materials/analysis tools: HZ QW XZ GY YL. Wrote the paper: HZ QW GY. Discussed the manuscript: HZ QW XZ GY YL.

References

1. Chapin III FS, Matson PPA (2011) Principles of terrestrial ecosystem ecology: Springer.
2. Wang KC, Dickinson RE (2012) A review of global terrestrial evapotranspiration: Observation, modeling, climatology, and climatic variability. Reviews of Geophysics 50: RG2005.
3. Jarvis PG, McNaughton K (1986) Stomatal control of transpiration: scaling up from leaf to region. Advances in ecological research 15: 49.
4. Wever LA, Flanagan LB, Carlson PJ (2002) Seasonal and interannual variation in evapotranspiration, energy balance and surface conductance in a northern temperate grassland. Agricultural and Forest Meteorology 112: 31–49.
5. Liu HZ, Feng JW (2012) Seasonal and interannual variations of evapotranspiration and energy exchange over different land surfaces in a semi-arid area of China. Journal of Applied Meteorology and Climatology 51: 1875–1888.
6. Seneviratne SI, Corti T, Davin EL, Hirschi M, Jaeger EB, et al. (2010) Investigating soil moisture–climate interactions in a changing climate: A review. Earth-Science Reviews 99: 125–161.
7. Lu N, Chen S, Wilske B, Sun G, Chen J (2011) Evapotranspiration and soil water relationships in a range of disturbed and undisturbed ecosystems in the semi-arid Inner Mongolia, China. Journal of Plant Ecology 4: 49–60.

8. Meinzer F, Hinckley T, Ceulemans R (1997) Apparent responses of stomata to transpiration and humidity in a hybrid poplar canopy. Plant, Cell & Environment 20: 1301–1308.
9. O'Grady A, Eamus D, Hutley L (1999) Transpiration increases during the dry season: patterns of tree water use in eucalypt open-forests of northern Australia. Tree Physiology 19: 591–597.
10. Zeppel MJB, Murray BR, Barton C, Eamus D (2004) Seasonal responses of xylem sap velocity to VPD and solar radiation during drought in a stand of native trees in temperate Australia. Functional Plant Biology 31: 461–470.
11. O'Brien JJ, Oberbauer SF, Clark DB (2004) Whole tree xylem sap flow responses to multiple environmental variables in a wet tropical forest. Plant, Cell & Environment 27: 551–567.
12. O'Grady AP, Worledge D, Battaglia M (2008) Constraints on transpiration of *Eucalyptus globulus* in southern Tasmania, Australia. Agricultural and Forest Meteorology 148: 453–465.
13. Chen L, Zhang Z, Li Z, Tang J, Caldwell P, et al. (2011) Biophysical control of whole tree transpiration under an urban environment in Northern China. Journal of Hydrology 402: 388–400.
14. Gwenzi W, Veneklaas EJ, Bleby TM, Yunusa IAM, Hinz C (2012) Transpiration and plant water relations of evergreen woody vegetation on a recently constructed artificial ecosystem under seasonally dry conditions in Western Australia. Hydrological Processes 26: 3281–3291.
15. Zheng C, Wang Q (2012) Water-use response to climate factors at whole tree and branch scale for a dominant desert species in central Asia: Haloxylon ammodendron. Ecohydrology DOI:10.1002/eco.1321.
16. Hu Z, Yu G, Zhou Y, Sun X, Li Y, et al. (2009) Partitioning of evapotranspiration and its controls in four grassland ecosystems: Application of a two-source model. Agricultural and Forest Meteorology 149: 1410–1420.
17. Jasechko S, Sharp ZD, Gibson JJ, Birks SJ, Yi Y, et al. (2013) Terrestrial water fluxes dominated by transpiration. Nature DOI:10.1038/nature11983.
18. Wang JL, Wen XF, Sun XM, Wang YY (2009) Asymmetry characteristic on the diurnal changes of CO_2 and H_2O fluxes at full heading time of winter-wheat in North China. Acta Agriculturae Boreali-Sinica 24: 159–163.
19. Unsworth MH, Phillips N, Link T, Bond BJ, Falk M, et al. (2004) Components and controls of water flux in an old-growth Douglas-fir-western hemlock ecosystem. Ecosystems 7: 468–481.
20. Zhang Q, Manzoni S, Katul G, Porporato A, Yang D (2014) The hysteretic evapotranspiration-vapor pressure deficit relation. Journal of Geophysical Research: Biogeosciences DOI:10.1002/2013JG002484.
21. Gu S, Tang YH, Cui XY, Du MY, Zhao L, et al. (2008) Characterizing evapotranspiration over a meadow ecosystem on the Qinghai-Tibetan Plateau. Journal of Geophysical Research 113: D08118.
22. Klein JA, Harte J, Zhao XQ (2004) Experimental warming causes large and rapid species loss, dampened by simulated grazing, on the Tibetan Plateau. Ecology Letters 7: 1170–1179.
23. Baldocchi D, Falge E, Gu L, Olson R, Hollinger D, et al. (2001) FLUXNET: a new tool to study the temporal and spatial variability of ecosystem-scale carbon dioxide, water vapor, and energy flux densities. Bulletin of the American Meteorological Society 82: 2415–2434.
24. Li YN, Zhao XQ, Cao GM, Zhao L, Wang QX (2004) Analyses on Climates and Vegetation Productivity Background at Haibei Alpine Meadow Ecosystem Research Station. Plateau Meteorology 23: 558–567.
25. Li YN, Zhao XQ, Wang QX, Gu S, Du MY, et al. (2003) The comparison of community biomass and environmental condition of five vegetation type in alpine meadow of Haibei, Qinghai Province. Journal of Mountain Science 21: 257–264.
26. Zhao L, Li YN, Gu S, Zhao XQ, Xu SX, et al. (2005) Carbon dioxide exchange between the atmosphere and an alpine shrubland meadow during the growing season on the Qinghai-Tibetan Plateau. Journal of Integrative Plant Biology 47: 271–282.
27. Li ZQ, Yu GR, Wen XF, Zhang LM, Ren CY, et al. (2004) Evaluation of the energy balance state of China flux observation network (China FLUX). Science in China Series D: Earth Sciences 34: 46–56.
28. Yu GR, Fu YL, Sun XM, Wen XF, Zhang L (2006) Recent progress and future directions of ChinaFLUX. Science in China Series D: Earth Sciences 49: 1–23.
29. Webb EK, Pearman GI, Leuning R (1980) Correction of flux measurements for density effects due to heat and water vapour transfer. Quarterly Journal of the Royal Meteorological Society 106: 85–100.
30. Reichstein M, Falge E, Baldocchi D, Papale D, Aubinet M, et al. (2005) On the separation of net ecosystem exchange into assimilation and ecosystem respiration: review and improved algorithm. Global Change Biology 11: 1424–1439.
31. Falge E, Baldocchi D, Olson R, Anthoni P, Aubinet M, et al. (2001) Gap filling strategies for defensible annual sums of net ecosystem exchange. Agricultural and Forest Meteorology 107: 43–69.
32. Priestley C, Taylor R (1972) On the assessment of surface heat flux and evaporation using large-scale parameters. Monthly weather review 100: 81–92.
33. Pan RZ (2008) Plant physiology (sixth edition). Beijing: Higher Education Press.
34. Eamus D, Cole S (1997) Diurnal and seasonal comparisons of assimilation, phyllode conductance and water potential of three Acacia and one Eucalyptus species in the wet–dry tropics of Australia. Australian Journal of Botany 45: 275–290.
35. Yu G, Nakayama K, Lu H (1996) Responses of stomatal conductance in field-grown maize leaves to certain environmental factors over a long term. Journal of Agricultural Meteorology 52: 311–320.
36. Wilson KB, Baldocchi DD (2000) Seasonal and interannual variability of energy fluxes over a broadleaved temperate deciduous forest in North America. Agricultural and Forest Meteorology 100: 1–18.